

## Electronic Supplementary Information

### Experimental Part

#### *Chemicals*

Polyacrylonitrile (PAN,  $M_w=150000$ , Sigma–Aldrich), poly(vinyl pyrrolidone) (PVP,  $M_w=1300000$ , Sigma–Aldrich), N, N-dimethylformamide (DMF, >99.5%, Sigma–Aldrich), tin(II) acetate ( $\text{Sn}(\text{CH}_3\text{COO})_2$ ,  $\text{Sn}(\text{Ac})_2$ , anhydrous, Sigma–Aldrich), and thiourea ( $\text{NH}_2\text{CSNH}_2$ ) were used without further treatments.

#### *Fabrication of SnS HNFs*

In a typical synthesis, 0.2 mmol  $\text{Sn}(\text{Ac})_2$  was dissolved in 20 mL DMF solution of 8 wt% PVP and 8 wt% PAN and stirred for 12 h. Then, the precursor solution was set on an electrospinning setup (New Era Pump Systems, Inc. USA) for nanofiber formation on aluminum foil under a voltage of 20 kV by using a high voltage power supply (Gamma ES50P-20W/DAM). The working distance between nozzle to collector was 20 cm and the flow rate was  $0.7 \text{ ml}\cdot\text{h}^{-1}$ . Afterwards, as-prepared PVP-PAN- $\text{Sn}(\text{Ac})_2$  NFs were heated in air at 600 °C for 2 h with a heating rate of  $3 \text{ }^\circ\text{C}\cdot\text{min}^{-1}$  to form SnO hollow nanofibers (SnO HNFs). After mixing with thiourea and heat-treating at 600 °C in nitrogen for 6 h with a heating rate of  $2 \text{ }^\circ\text{C}\cdot\text{min}^{-1}$ , SnO HNFs were converted into SnS HNFs. Finally, the SnS HNFs were washed with water and ethanol three times, respectively.

#### *Structural and morphological characterization*

The morphology of SnO HNFs and SnS HNFs was investigated by scanning electron microscopy (SEM, FEI VERIOS 460L) and transmission electron microscopy (TEM, Hitachi HF 2000, at accelerating voltage of 200 kV). Wide-angle X-ray diffractometer (WAXD, Rigaku Smartlab) was employed to study the lattice structure of SnS HNFs. Nitrogen adsorption–desorption measurements of SnO HNFs and SnS HNFs were carried out on an ASAP 2020 surface characterization analyzer (Micromeritics

Instrument, USA). The sample quality was kept as 0.1g in each test to ensure the accuracy of the test result. Before measurement, all samples were degassed at 110 °C under vacuum for 20 h. The pore parameters such as specific surface area, pore size distribution, and pore volume were obtained according to the nitrogen adsorption–desorption isotherms at 77 K. The specific surface area values of these samples were acquired by using the Brunauer–Emmett–Teller (BET) method. The pore size distribution profiles from the nitrogen adsorption branch of isotherms were obtained by applying a non-local density functional theory (NLDFT) and a carbon slit pore model. The total pore volume was calculated from the amount of nitrogen adsorbed at the relative pressure of  $P/P_0=0.97$ .

### ***Electrochemical tests***

For electrode preparation, a homogenous slurry was obtained through mixing the synthesized active material (SnS HNFs) with carbon black and alginic acid sodium salt (8: 1: 1 in weight) in deionized water, and then it was casted on a copper foil, followed by drying under vacuum oven overnight. The sodium coin cells (CR2032-type) were assembled in a pure Ar-filled glove box, using Na metal as the counter electrode and glass fiber (Whatman GF/D) as the separator. The electrolyte was 1 M  $\text{NaClO}_4$  in a solvent mixture of ethylene carbonate, propylene carbonate, and fluoroethylene carbonate (EC/PC/FEC), with a volume ratio of 10:10:1. Cyclic voltammetry (CV) measurements were carried out by Gamry Reference 600 system at a scan rate of  $0.1 \text{ mV}\cdot\text{s}^{-1}$  in a voltage range of 0.01–2.5V against sodium. Electrochemical impedance spectroscopy (EIS) tests were performed within a frequency range of 0.01 Hz-100 kHz by the same equipment. Moreover, the cells were galvanostatically discharged and charged in a voltage range of 0.01–2.5 V using a LAND (CT2001A) battery testing system. All capacity values were calculated based on the total weight of the SnS HNF anode.

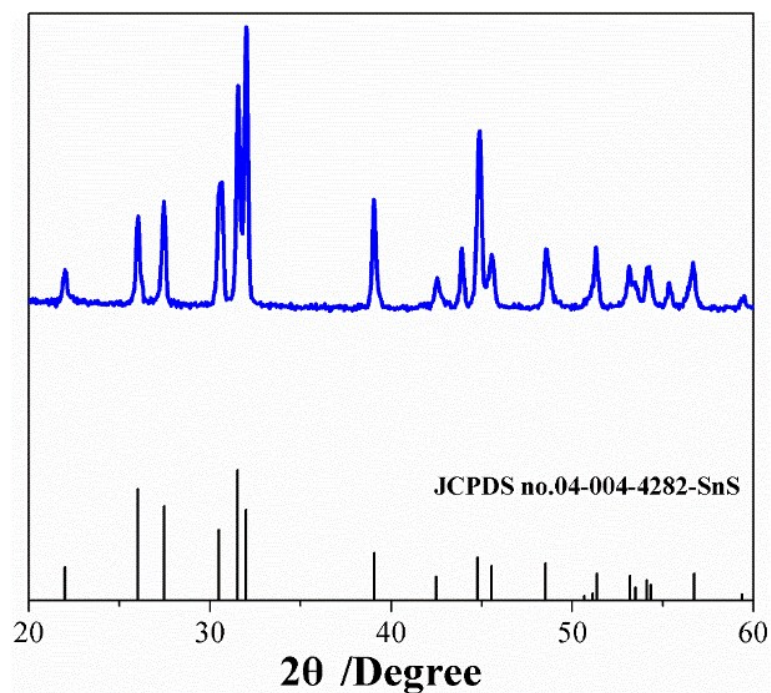


**Fig S1.** XRD patterns of SnS HNFs.

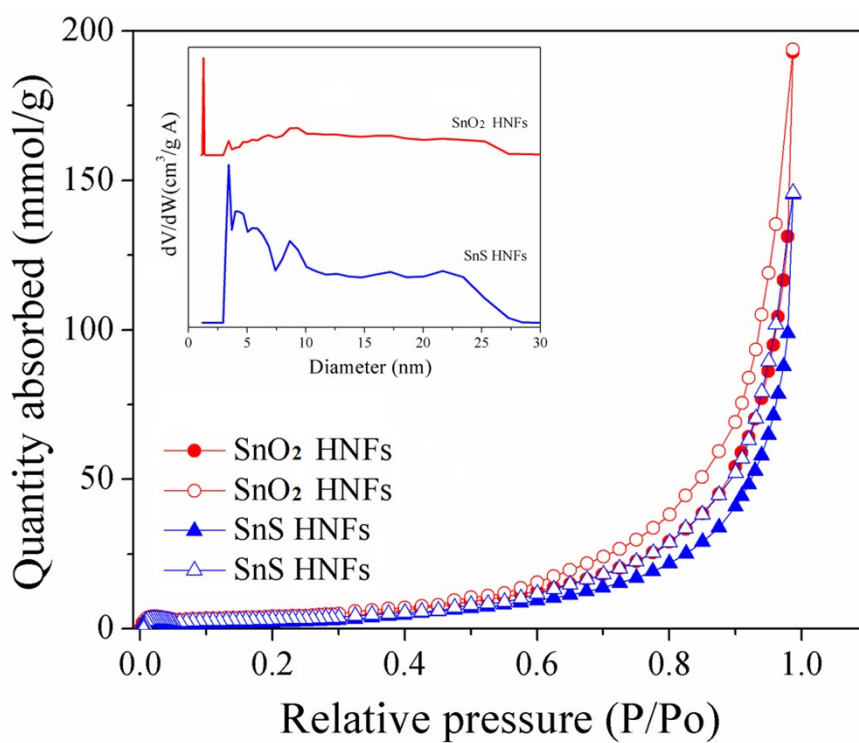


**Fig S2.** BET plots and corresponding pore size distributions (inserted) of SnO<sub>2</sub> HNFs and SnS HNFs

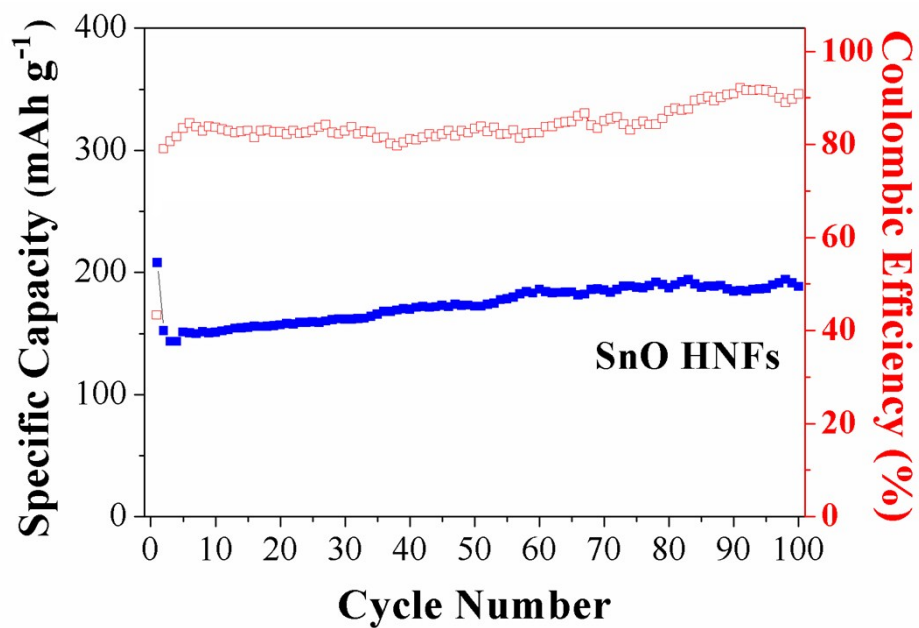


**Fig. S3.** Cycling performance of  $\text{SnO}_2$  HNFs under  $100 \text{ mA}\cdot\text{g}^{-1}$

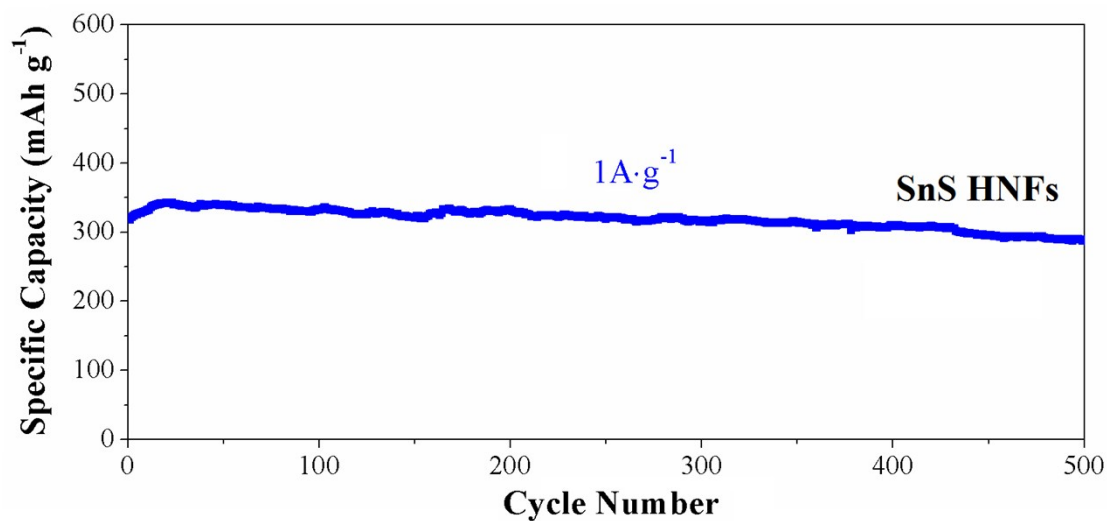


**Fig. S4.** Cycling performance of SnS HNFs under  $1 \text{ A}\cdot\text{g}^{-1}$

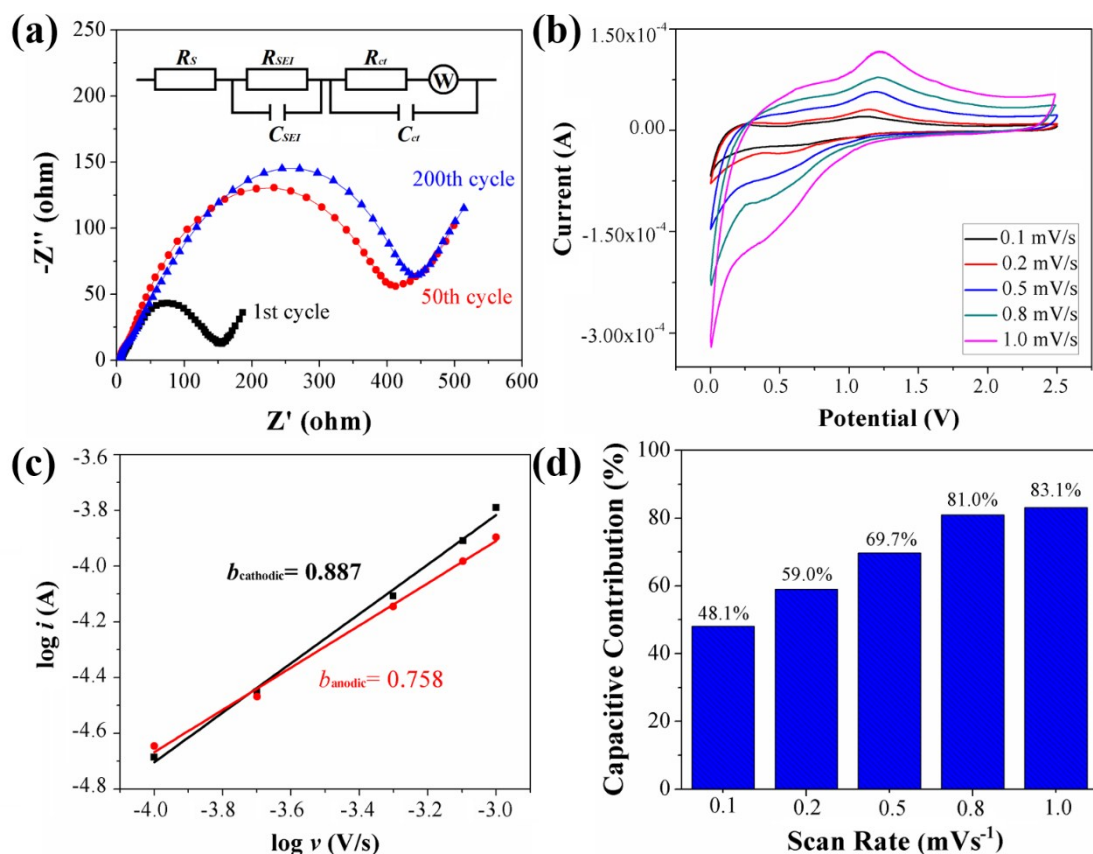


**Fig. S5.** (a) EIS spectra of SnS HNFs, (b) CV curves of SnS HNFs at different scan rates, (c)  $\log(i)$  vs  $\log(v)$  plots of cathodic ( $\sim 0.55$  V) and anodic ( $\sim 1.4$  V) peaks, and (d) Pseudocapacitive contribution of SnS HNFs under different scan rates.

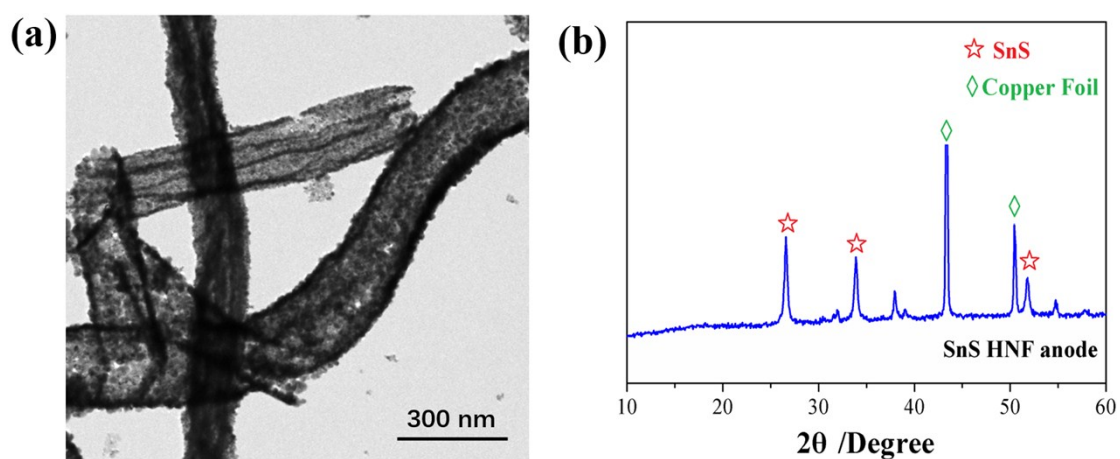


**Fig. S6.** TEM image (a) and XRD patterns (b) of SnS HNFs after 100 cycles at  $100 \text{ mA} \cdot \text{g}^{-1}$ .